



# HHS Public Access

Author manuscript

*Nanomedicine*. Author manuscript; available in PMC 2016 November 01.

Published in final edited form as:

*Nanomedicine*. 2015 November ; 11(8): 1893–1907. doi:10.1016/j.nano.2015.07.015.

## Design considerations for nanotherapeutics in oncology

Triantafyllos Stylianopoulos<sup>1</sup> and Rakesh K. Jain<sup>2</sup>

<sup>1</sup>Cancer Biophysics Laboratory, Department of Mechanical and Manufacturing Engineering, University of Cyprus, 1678, Nicosia, Cyprus

<sup>2</sup>Edwin L. Steele Laboratories, Department of Radiation Oncology, Massachusetts General Hospital and Harvard Medical School, 02114, Boston, MA, USA

### Abstract

Nanotherapeutics have improved the quality of life of cancer patients, primarily by reducing the adverse effects of chemotherapeutic agents, but improvements in overall survival are modest. This is in large part due to the fact that the Enhanced Permeability and Retention effect, which is the basis for the use of nanoparticles in cancer, can be also a barrier to the delivery of nanomedicines. A careful design of nanoparticle formulations can overcome barriers posed by the tumor microenvironment and result in better treatments. In this review, we first discuss strengths and limitations of clinically-approved nanoparticles. Then, we evaluate design parameters that can be modulated to optimize intratumoral delivery. The benefits of active tumor targeting and drug release rate on intratumoral delivery and treatment efficacy are also discussed. Finally, we suggest specific design strategies that should optimize delivery to most solid tumors and discuss under what conditions active targeting would be beneficial.

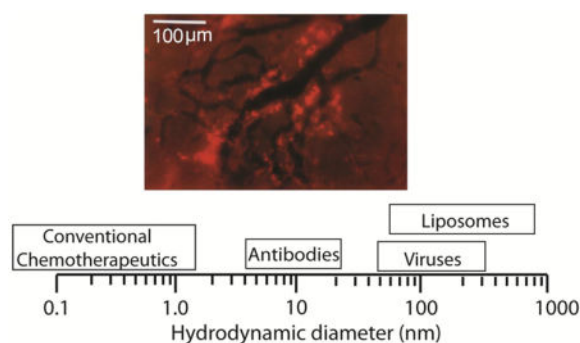
### Graphical Abstract

---

Corresponding authors: Triantafyllos Stylianopoulos, Tel: +357 2289.2238, Fax: +357 2289.5081, [tstylian@ucy.ac.cy](mailto:tstylian@ucy.ac.cy). Rakesh K. Jain, Tel: 617.726.4083, Fax: 617.724.1819, [jain@steele.mgh.harvard.edu](mailto:jain@steele.mgh.harvard.edu).

Conflict of interests: R.K.J. received research grants from Dyax, Med Immune and Roche; consulting fees from Enlight, Ophthotech, SPARC and SynDevRx; owns equity in Enlight, Ophthotech, SynDevRx and XTuit, serves on the Board of Directors of XTuit and Board of Trustees of Tekla Healthcare Investors, Tekla Life Sciences Investors, Tekla Healthcare Opportunities Fund and Tekla World Healthcare Fund. No reagents or funding from these companies was used in these studies. Therefore, there is no significant financial or other competing interest in the work.

**Publisher's Disclaimer:** This is a PDF file of an unedited manuscript that has been accepted for publication. As a service to our customers we are providing this early version of the manuscript. The manuscript will undergo copyediting, typesetting, and review of the resulting proof before it is published in its final citable form. Please note that during the production process errors may be discovered which could affect the content, and all legal disclaimers that apply to the journal pertain.



Barriers posed by the abnormal tumor micro-environment hinder delivery of nanoparticles to solid tumors, causing heterogeneous drug distribution and reducing the efficacy of the treatment. Careful design of the physicochemical properties of nanoparticles as well as their binding affinity to cancer cells and the controlled release of the drug can improve delivery and treatment outcomes. In this review, design considerations are provided for nano-therapeutics in oncology. Image shows heterogeneous intratumoral distribution of liposomes (bright red color) 90 nm in diameter (with permission from Yuan, F. *et al. Cancer Res.* 54, 3352–3356, 1994)

## Keywords

nanomedicine; EPR effect; controlled drug release; nanoparticle targeting; cancer therapy

## Introduction

The selective accumulation of nanoparticles in tumors is attributed to the hyper-permeability of the tumor blood vessels that enables nano-scale molecules and particles to preferentially enter the tumor interstitial space and the dysfunction of intratumoral lymphatics that allow particles to stay in the tumor for a longer time<sup>1–3</sup>. This Enhanced Permeability and Retention (EPR) concept was first introduced in 1986 by two independent studies by Jain<sup>4</sup> and Maeda<sup>5</sup>. Both studies stressed the potential benefit of the use of nanotherapeutics in cancer. In subsequent years, the fact that EPR can also pose a barrier to the effective delivery of large therapeutic agents was also highlighted<sup>1,6–8</sup>. Indeed, hyper-permeable tumor blood vessels can cause excessive fluid loss from the vascular to the interstitial space of the tumor, which reduces tumor perfusion and thus, can hinder the systemic delivery of nanoparticles<sup>9–11</sup>. Furthermore, the hyper-permeability of the tumor vessels often results in uniformly elevated interstitial fluid pressure, which becomes comparable to the microvascular pressure and eliminates pressure differences across the tumor vessel wall and in the tumor interior<sup>12–14</sup>. As a result, transvascular and interstitial flows diminish and thus, diffusion becomes the main mechanism of nanoparticle transport. Since diffusion decreases with the size of the drug, extravasation of large particles as well as intratumoral distribution is hindered<sup>4,15–18</sup>. Despite these limitations in the use of nanoparticles to treat cancer, the first nanotherapeutic – Doxil – was approved for clinical use in 1995<sup>19</sup> and since then more cancer nanomedicines have entered the market,<sup>20–24</sup> which highlights the potential impact that nanomedicine can have on cancer therapy.

## Cancer nanomedicines in clinical use and in trials

Currently, clinically approved cancer nanomedicines make use of the EPR effect, i.e., passive accumulation into the tumor, and include (Figure 1): Doxil (or Caelyx) - an ~100 nm pegylated liposomal doxorubicin particle - approved for the treatment of HIV-related Kaposi's sarcoma, metastatic ovarian cancer and metastatic breast cancer; DaunoXome - a 50 nm liposomal daunorubicin particle - approved for HIV-related Kaposi's sarcoma; Myocet - an 150–180 nm non-pegylated liposomal doxorubicin particle approved in Europe and Canada for metastatic breast cancers; Abraxane - a 10nm albumin-bound paclitaxel particle (following disintegration in plasma) - approved for metastatic breast cancer and recently for pancreatic ductal adenocarcinoma; Lipusu - a liposomal paclitaxel particle - approved in China for various cancers including breast cancers and non-small-cell lung cancer; Genexol-PM - a 20–50 nm Cremophor-free, polymeric micelle-formulated paclitaxel - approved in South Korea for metastatic breast cancer; MM-398 - an ~ 100 nm liposomal formulation of irinotecan - approved recently for the treatment of pancreatic ductal adenocarcinoma; and finally, PICN - a 100–110 nm formulation of paclitaxel stabilized with polymer and lipids - approved in India for metastatic breast cancer and currently in clinical trials in the US (Table 1).

As shown in Table 1, the major advantage of the clinically approved nanoparticle formulations compared to conventional chemotherapy is that they are associated with significantly less adverse effects, and in most cases toxicities are different from those of the active drug. In some cases, these nanoparticles were developed to reduce specific severe adverse effects of chemotherapy. For instance, doxorubicin is known to cause cardiotoxicity in breast cancer patients. Encapsulation of the drug in a liposomal formulation, such as in Doxil or Myocet, decreased the amount of the drug that was delivered to the heart and thus, ameliorated cardiotoxicity significantly<sup>27</sup>. In another case, taxanes, namely paclitaxel and docetaxel, are administered with synthetic solvents to enhance solubility. Specifically, paclitaxel contains castor oil (Cremophor EL) and docetaxel contains polysorbate 80. These solvents directly contribute to severe toxicities including hypersensitivity reactions and peripheral neuropathy. Abraxane and PICN have the ability to cause limited hypersensitivity reactions<sup>30,36</sup>. Apart from reducing severe adverse effects, encapsulation of chemotherapy into nanocarriers can improve the pharmacokinetics of the therapeutic agent and particularly the blood circulation time. In general, the longer the drug stays in the circulation, the better are the chances to extravasate into the tumor through the EPR effect, but at the same time it should not extravasate to normal tissues. Remarkably high circulation times are achieved with Doxil, due to the pegylation of its outer surface that prevents interactions with serum proteins<sup>23</sup>.

Nanoparticle formulations currently in clinical trials are shown in Table 2. The advances in nanotechnology have introduced a large variety of nanoparticle formulations, which includes: polymers (e.g. micelles), dendrimers, liposomes, quantum dots, gold and silica particles as well as magnetic and carbon-based formulations<sup>23,37</sup>. Tables 1 and 2, respectively, list the liposomes and polymer particles that have, thus far, been approved and are in clinical trials<sup>38</sup>. Furthermore, MCC-465, SGT-53, BIND-014 and CALAA-01 contain targeting ligands for preferential binding to cancer cells. Specifically, MCC-465 is

tagged with the F(ab')<sub>2</sub> fragment of human monoclonal antibody GAH, which preferentially binds to neoplastic stomach tissues<sup>39</sup>; SGT-53 utilizes an anti-transferrin single-chain antibody fragment (scFv) that targets to cancer cells through the transferrin glycoprotein receptor, which is highly expressed in many cancer cells<sup>40</sup>; BIND-014 contains the ACUPA moiety, a targeting ligand that mediates molecular interactions between nanoparticles and prostate specific membrane antigens (PSMA) expressed on prostate cancer cells and in non-prostate solid tumor neovasculature<sup>41</sup> and CALAA-01 contains human transferrin as a targeting ligand for binding to transferrin receptors, which as mentioned earlier is upregulated on cancer cells<sup>42,43</sup>. Nanoparticle targeting to cancer cells can be beneficial for the delivery and treatment efficacy of the drug, but as we discuss later in this review, in certain circumstances it might inhibit uniform distribution of the drug in the tumor. The size of the nanoparticles presented in Table 2 is in the range of 20 – 150 nm, similar to the size of the clinically approved particles. Binding affinity and particle size are important parameters for the delivery of nanoparticles as well as particle surface charge, shape and drug release rate. In the following sections, we discuss how these parameters affect delivery to and within the tumor and propose design strategies for improving treatment.

## Design considerations

Delivery of blood-borne therapeutic agents to solid tumors is determined by the circulation time of the particles within the vascular network, the ability of the particles to cross the tumor vessel wall into the tumor interstitial space, the interstitial transport of the particles within the tumor and finally, their ability to bind to cancer cells, release the drug that can get internalized by cancer cells<sup>3,8</sup>.

## Vascular transport

Systemically administered nanoparticles - provided they are not toxic - should be able to circulate in the blood for a long time to have higher chances to reach the tumor vasculature and extravasate into the tumor tissue. At the same time, these nanoparticles should not cross the vessel wall of normal tissues and cause adverse effects. The pore cut off size of the normal vessel wall is in the range of 6–12 nm<sup>46</sup>, which suggests that nanoparticles should be larger than this size range. Additionally, clearance from the blood circulation is performed by filtration in the kidneys or by the reticuloendothelium system in the liver and the spleen. Renal clearance is very rapid for particles with hydrodynamic diameter smaller than 5–6 nm, while clearance by the liver and the spleen is rapid for large particles, above 200 nm in diameter<sup>47–50</sup>. For nanoparticles within the range of 6 to 200 nm, studies have shown that blood half-life decreases as the particle diameter increases, provided the surface chemistry remains the same<sup>51,52</sup>.

As far as the particle shape is concerned, filamentous micelles have circulation times about ten times longer than their spherical counterparts, while nanotubes with diameters less than 2nm have rapid clearance from the kidneys, which reduces drastically their circulation times<sup>53,54</sup>. However, nanorods 15 nm in diameter and with an aspect ratio of approximately 4, have shown similar circulation times to spherical particles of equal hydrodynamic radius (35 nm), suggesting that elongated particles with diameters above 10 nm cannot be cleared easily from the vascular network<sup>55</sup>. Finally, surface chemistry and charge density play a

crucial role for the vascular transport of nanoparticles. The higher the charge of the particles (anionic or cationic), the greater their clearance from the reticuloendothelial system<sup>50</sup>. Furthermore, cationic particles induce opsonization, i.e., binding of plasma proteins to their surface that signals immune cells<sup>56</sup>. Hence, it would be preferable for the nanoparticle formulations to have a near neutral charge.

A common practice of surface functionalization is the passivation of the particle by adding a neutral layer of polyethylene glycol (PEG) to its surface (PEGylation)<sup>57,58</sup>. PEGylation prevents opsonization and phagocytosis by the cells of the reticuloendothelium system (e.g. Kupfer cells, phagocytes, etc.) creating “stealth” nanoparticles and allowing long circulation times. The molecular weight and PEG density of the coating are determinant factors for the efficiency of PEGylation. PEG molecular weight ranging from 2000 to 5000 g/mol was found to cause maximal reduction in protein adsorption when it was applied to relatively large polymeric particles with a size range of 160–270 nm<sup>59</sup>. The ideal density of PEG is highly dependent on the material the nanoparticle is made of<sup>60,61</sup>. Except for PEG, other hydrophilic and neutral polymers have been also used to prolong blood circulation times, including zwitterionic and carbohydrate coatings<sup>62,63</sup>.

In conclusion, PEGylated nanoparticles with a hydrodynamic diameter above 12 nm but less than 200 nm can in general ensure sufficient circulation times and seem to selectively reach tumors.

### Transvascular transport

The transport of nanoparticles across the tumor vessel wall and into the interstitial space of the tumor is the transport step that the EPR effect is associated with. The primary design condition is that particles should be able to pass through the pores of the leaky tumor vessels but not the pores of the normal vessels. As mentioned above, in normal tissues the pore cut off size of the vessel wall ranges from 6 to 12 nm<sup>46</sup>. This is the largest size of proteins, molecules and particles in the blood that can cross the vessels wall and thus, in order for nanoparticles to selectively accumulate in the tumor tissue they should have a size larger than that. Transvascular transport depends on the difference between the microvascular and interstitial fluid pressure as well as the interactions between the particle and the vessel wall<sup>1,17</sup>. The interstitial fluid pressure is in large part controlled by the permeability of the vessels and by lymphatic dysfunction. Some tumors have large intercellular openings in the endothelial lining<sup>64</sup>. In this case, excessive fluid flows from the vascular to the interstitial space and insufficient drainage due to the dysfunctional lymphatic system causes the accumulation of the fluid in the tumor and the elevation of the interstitial fluid pressure. As a result, the interstitial fluid pressure can be as high as the microvascular pressure, which eliminates pressure differences and the only mechanism of transport is diffusion - a mechanism that is inversely related to the size of the particles (Figure 2A)<sup>1,13,14,65–67</sup>.

The interactions between the particle and the openings of the tumor vessel wall can be of three types: steric due to collisions of the particle with the wall, hydrodynamic due to hydrodynamic forces induced by the motion of the particle within the fluid medium, and electrostatic due to electrostatic repulsion or attraction between charged particles and the negatively charged glycocalyx on the surface of the vessel wall<sup>17,68,69</sup>. All these types of

interactions are controlled by the relative size of the particle to the openings of the wall<sup>69</sup>. The smaller this ratio, the less important the effect of the interactions becomes, and the transport is not hindered. Whereas as the particle size approaches the size of the openings, the interactions become more important, the transport is hindered and finally the particle will not be able to pass through the wall. Our calculations<sup>17</sup> suggest that neutral particles with a diameter larger than 60% of the openings of the vessel wall will be excluded due to steric interactions.

From the above analysis we conclude that for very permeable tumors (e.g., openings larger than 200 nm) the transport of particles of all sizes will be hindered due to the elevated interstitial fluid pressure. For less permeable tumors, there will be a pressure difference across the vessel wall, which will enhance the penetration of the particles but as the size of the openings becomes smaller even though the pressure difference increases, large particles might be excluded due to interactions with the vessel wall. Therefore, there is a size-dependent delivery of nanoparticles from the tumor vasculature into the interior of the tumor, which will benefit only small particles with sizes usually less than 60 nm (Figure 2B)<sup>16–18,70</sup>. Therefore the transport of particles larger than 60 nm, such as Doxil, will be always limited, while the transport of smaller particles can be optimized for low or moderately permeable tumors. Note that even though MM-398 is of the same size as Doxil, it has been clinically approved for the treatment of pancreatic ductal adenocarcinomas, which are considered to be poorly permeable<sup>10,71</sup>. The potency and release rate of the drug as well as the number of drug molecules a nanoparticle can carry (i.e., load capacity) are equally important design parameters that determine the uniform distribution of the drug into the tumor and thus, the efficacy of the nanoparticle formulation. Other nanoparticles whose efficacy depends on controlled drug release include IMMU-130, an anti-CEA-SN38 conjugate, which does not internalize into cancer cells but releases SN-38 that attacks cancer cells<sup>72</sup> and antibody drug conjugates that target cancer cells or tumor stromal components (collagen, fibrin) and then release the therapeutic load in a controlled fashion<sup>73</sup>.

Electrostatic interactions depend not only on the relative size of the particles versus the pores but also on the distance around the particle that these interactions become important (i.e., the Debye length). For physiological conditions (ionic strength 0.15 M) the Debye length is 1–2 nm and thus, only when the particles come very close to the wall, they will interact. As a result, electrostatic repulsions of anionic particles with the negatively charged vessel wall are usually not very important and thus, transvascular transport is not affected considerably. Electrostatic attraction of cationic particles to the vessel wall might, however, increase transvascular transport because the particles from the blood vessels come closer to the vessel wall and have a higher propensity to extravasate (Figure 2C). Notice, that because these particles travel with the velocity of the fluid, some of them might not bind to the vessel wall and go through the wall openings into the tumor interstitial space. Indeed, experimental and theoretical studies have shown that cationic nanoparticles have superior transvascular flux compared to their anionic or neutral counterparts<sup>69,74–78</sup>. Furthermore, studies using zwitterionic quantum dot particles have shown that the spatial configuration of the surface charge plays also a role in the amount of the particles that crosses the vessel wall<sup>79</sup>. Specifically, when surface modification includes both anionic and cationic molecules (e.g.,

carboxylate and sulfonate groups), transport is enhanced when the cationic group is exposed to the tumor vessel wall.

As far as the effect of particle shape is concerned, transvascular flux of elongated particles, such as nanorods, is superior compared to spherical particles of equal hydrodynamic diameter (Figure 2D,E) <sup>55,80</sup>. This could be explained by the fact that non-spherical particles traveling in the blood stream interact more actively with the vessel wall as they exhibit tumbling and rolling motions <sup>81</sup>. Therefore, elongated nanoparticles have a higher probability to be in the proximity of the vessel wall and cross it. In addition, even though it has not been elucidated yet, we speculate that steric and hydrodynamic interactions are lower for elongated particles. These interactions might become more complex for hollow particles such as carbon nanotubes, which is expected to hinder transvascular transport <sup>82</sup>.

In conclusion, spherical nanoparticles with diameters in the range of 12 – 60 nm, elongated particles with similar hydrodynamic diameters and cationic particles are likely to have superior extravasation into the tumor tissue.

### Interstitial transport

Similar to transvascular transport, interstitial transport is controlled by the gradients of the interstitial fluid pressure within the tumor as well as by steric, hydrodynamic and electrostatic interactions between the particles and the openings (pores) of the interstitial space (Figure 3A) <sup>83–85</sup>. Interstitial fluid pressure is uniformly elevated in the interior of the tumor eliminating any pressure difference and rendering diffusion the main mechanism of transport. Furthermore, in the periphery of the tumor, the fluid pressure drops rapidly to normal values creating a steep pressure gradient, which can push nanoparticles concentrated in the periphery of the tumor into the surrounding tissues <sup>66,86,87</sup>.

Diffusion is inversely proportional to particle size and it depends on the interactions of the particles with the extracellular fibers (Figure 3B). When the particle size is much smaller than the size of the interstitial pores (e.g., for low fraction of fibers or for small size drugs such as chemotherapeutic agents) steric and hydrodynamic interactions are not important <sup>85,88</sup>. However, the desmoplastic response observed in many tumors overproduces extracellular fibers and the pores can be on the order of 100 nm or smaller. As a result, particles or macromolecules with a hydrodynamic diameter larger than 50 nm might not be able to effectively and uniformly diffuse in the tumor interstitial space <sup>83,89–91</sup>. Therefore, even if nanoparticles are able to cross the hyper-permeable tumor vessels, they might not be able to penetrate deep into the tumor interior, and thus, concentrate in the perivascular regions <sup>51,92</sup> or end up to the surrounding normal tissue if the particles are concentrated at the tumor periphery, as discussed in the previous paragraph. In these cases, the efficacy of the nanoparticles depends largely on the drug release rate, which also determines the distribution of the drug into the tumor. In contrast, the diffusivity of particles smaller than 5 nm is minimally hindered <sup>83</sup> and thus, these nanoparticles should be able to effectively diffuse into the tumor tissue. Therefore, nanoparticles with a diameter in the range of 5 to 50 nm would, in general, distribute more homogeneously within the tumor <sup>51,52</sup>.

Electrostatic interactions also play a crucial role in the intratumoral distribution of nanoparticles. Collagen fibers have a slightly positive charge, while hyaluronic acid has a high negative charge. Therefore, both cationic and anionic particles will develop electrostatic repulsion and attraction with charged fibers<sup>84,93</sup>. The magnitude of these forces is governed by the Debye length. As mentioned earlier, for physiological conditions this length is 1–2 nm, and thus, particles have to come very close to the fibers to sense any electrostatic forces. In the case of oppositely charged fibers, when a particle approaches the fibers within a distance of a few Debye lengths, it is likely to stick to the fibers and form aggregates<sup>93</sup>. Electrostatic repulsions even though hinder the diffusivity of the particle cannot drastically affect the diffusion (Figure 3C)<sup>84</sup>. Therefore, neutral particles can more homogeneously distribute in the tumor compared to their cationic or anionic counterparts.

As with the transport through the openings of the tumor vessel wall, non-spherical particles and macromolecules can more effectively diffuse into the extracellular space of the tumor compared to spherical particles of equal hydrodynamic diameter (Figure 3D)<sup>55</sup>. Elongated particles should exhibit lower steric and hydrodynamic interactions with the fibers and diffuse faster in the direction of their long axis. A distinction should be made, however, between rigid and flexible nano-sized rods, as the latter would have a different diffusion mechanism and exhibit greater diffusivities than rigid rods or spheres of similar hydrodynamic size<sup>94</sup>.

In conclusion, spherical particles with a diameter of 5 – 50 nm, elongated particles with similar hydrodynamic diameters and neutral particles are ideal to optimize nanoparticle penetration in the tumor interstitial space. Obviously, there is a better penetration for smaller particles, but very small particles might be cleared rapidly from the tumor tissue due to limited retention. As discussed earlier for transvascular transport, the efficacy of particles larger than 50 nm will depend on the release kinetics of drugs from these particles.

### Intracellular transport

Efficient and homogeneous distribution of nanomedicines in solid tumors is directly related to better treatment outcome<sup>17</sup>. Some nano-scale drugs might, however, require intracellular delivery, while others could release the anti-cancer agents once they are in the tumor microenvironment. In the former case, the efficacy of nanotherapy might be further improved by accounting for the effects of size, surface charge and shape on cellular internalization. For spherical particles, it has been shown that particle size might determine the mechanism of internalization and the amount of nanoparticle uptake<sup>95</sup>. Indeed, researchers have found both experimentally and with the use of mathematical modeling that internalization is maximized for a range of particle sizes<sup>96–98</sup>. For gold and silver nanoparticles in the size range of 2–100 nm, particles of sizes 40–50nm were able to more effectively bind and induce receptor-mediated endocytic processes<sup>99</sup>. Additionally, it has been shown that nanoparticles with a size larger than 50 nm are more likely to be excluded from the cell nucleus<sup>100</sup>.

As far as particle surface charge is concerned, cationic particles seem superior compared to neutral or anionic particles, even though the results are still not conclusive<sup>101,102</sup>. The cellular membrane is covered with negatively charged sulfated proteoglycans, which attract



cationic particles<sup>103</sup>. As a result, *in vitro* experiments have shown that cationic nanoparticles outperform their anionic counterparts<sup>101,102</sup>. Surface charge might also determine the uptake mechanism<sup>104</sup>.

Finally as for the particle shape, it has been shown that for particles less than 100 nm in size, spherical nanoparticles are internalized more effectively than rod shaped, elongated particles<sup>98</sup>. For larger sizes, however, internalization is faster and more efficient for elongated particles (high aspect ratio)<sup>105</sup>. Additionally, the local geometry of the particle at the contact point with the cell determines whether it will be internalized or not<sup>106</sup>. Specifically, internalization is more effective when rod-like particles align perpendicular to the cellular membrane as opposed to parallel alignment, carrying a positive charge. It should be noted, however, that many of the particles used in these studies were in the micro-meter size range, much larger than the formulations used in nanomedicine and most of the findings are based on *in vitro* experiments, which might be different from the *in vivo* situation. Thus, the relevance of shape in cellular internalization of nanoparticles *in vivo* remains to be shown.

In conclusion, further studies are required to better understand the effect of particle's physical properties on cellular uptake. Moreover, nanoparticles that release their therapeutic load once they enter the tumor microenvironment do not need to be internalized.

## Multifunctional and stimuli-responsive drug delivery systems

Nanoparticle delivery systems apart from acting as drug-carriers might have other functions as well<sup>107</sup>. Such functions often involve the controlled release of the therapeutic agent from the nanoparticle, employment of targeting agents (e.g., antibodies, peptides) for specific binding of the particles to cancer cells or other target in the tumor microenvironment or an imaging agent for diagnostic purposes<sup>108–114</sup>. Furthermore to trigger drug release, nanoparticles might be responsive to a stimulus in the tumor microenvironment (e.g. pH, temperature, redox, enzyme activity) or a stimulus applied externally to the tumor (e.g. heat, light, magnetic field, ultrasound)<sup>112,115–119</sup>. These multifunctional nanoparticle systems are promising because they can perform several therapeutic and diagnostic tasks simultaneously and trigger local release in the tumor tissue. Careful design of their properties is, however, required so that delivery is optimal. In addition, increased sophistication is likely to result in an increase in the size of the particle, which will hinder its transport across the tumor vessel wall and its penetration into the tumor interstitial space. From the nanoparticle formulations currently in clinical trials (Table 2), MCC-436, SGT-53, BIND-014 and CALAA-01 aim to selectively target cancer cells with targeting agents, while Thermodox is a heat activated liposome containing doxorubicin. Targeting elements can also be specific peptides that interact with the tumor vasculature and tissue to enhance nanoparticle penetration. Tumor-penetrating peptides used to enhance nanoparticle delivery include iRGD, NGR, LyP-1, and F3<sup>120</sup>. Nanoparticle formulations successfully tested with penetration peptides include doxorubicin liposomes, Abraxane, micelles, iron oxide particles, quantum dots and hydrogels<sup>121–126</sup>.

## Targeted nanomedicines: the interplay among interstitial diffusion, drug release rate and binding affinity

For the case of targeted nanoparticles, additional design considerations are necessary. Once the nanoparticle enters the tumor interstitial space, a competition of three mechanisms determines its efficacy: i) the penetration of the nanoparticle into the tumor, described primarily by its interstitial diffusivity,  $D$  ii) the rate of release of the anti-cancer drug, described by the release rate constant,  $K_{rel}$ , and iii) the binding affinity of the nanoparticle or the released drug to cancer cells, described by the binding rate constant  $K_{on}$  (Figure 4A,B). A very rapid release of the drug before the nanoparticles have penetrated deep into the tumor might cause heterogeneous drug distribution, while a very slow release might result in most of the nanoparticles to have already cleared from the tumor. Furthermore, a very high binding affinity of the nanoparticles will result in accumulation near the blood vessels, from which nanoparticles have extravasated. Finally, it is also possible for the released drug to bind rapidly to cells, which causes nonuniform and incomplete intratumoral distribution<sup>127</sup>. The delivery barrier due to high binding affinity of the drug or the nanoparticle is also known as the “binding-site barrier”, which poses limitations for cancer cell targeted nanoparticles<sup>128–130</sup>. By including effects of nanoparticle transport and binding and the release of the drug, we estimated that the penetration of nanoparticles from tumor blood vessels would decrease with the distance from the vessel wall,  $x$ , exponentially approximately as  $Ae^{-x/L_i}$ , with a characteristic length scale,  $L_i$ , given by<sup>131</sup>

$$L_i = 2D / \left[ \left( v^2 + 2K_i D \right)^{0.5} - v \right],$$

$K_i$  is the release or binding rate constant,  $D$  the diffusion coefficient and  $v$  is the interstitial fluid velocity of the interstitial space. In the interior of solid tumors, the uniformly elevated fluid pressure often eliminates interstitial flow and thus, the characteristic lengths become  $L_i = (D/K_i)$ . This equation highlights the competition between interstitial diffusion and binding and/or drug release rate. The distance to which the nanoparticle penetrates from the vessel wall can be estimated by the characteristic lengths with longer lengths generally providing more uniform drug distribution, but potentially at the cost of lower concentrations of the drug. Based on these considerations, we conclude that deep penetration into the tumor requires either a high diffusion coefficient (i.e., small size particle) or a low drug release rate and binding affinity of the nanoparticle or the drug.

These results reconcile the contradictory experimental data regarding the effect of nanoparticle targeting to cancer cells on their therapeutic outcome<sup>24,132,133</sup>. Specifically, some preclinical and clinical studies have shown that antibody-conjugates and nanoparticles equipped with targeting moieties to recognize and bind to cancer cells increased intratumoral penetration and efficacy<sup>41,43,45,122,123,134</sup>. In contrast, other studies suggest that nanoparticle binding increases intracellular drug accumulation but not the intratumoral distribution and the efficacy of the drug<sup>133,135,136</sup>.

Apart from the drug release rate and affinity, the loading capacity of a nanoparticle is another parameter that should be taken into account. Obviously, the higher the efficiency of a nanoparticle to encapsulate cytotoxic agents the better its efficacy is expected to be. Except for the type of the drug, design parameters that affect loading capacity are the size of the particle, the material that it is made of and the mechanism of entrapment (i.e., physical entrapment, coordinate bonding, chemical conjugation, etc.). Larger nanoparticles of the same material have been found to have a higher drug content and efficiency<sup>137</sup>, without this being a general rule<sup>138</sup>. For instance, in the case of polymeric micelles, Genexol-PM has a size of 20–50 nm, and loading capacity of 16.7%, NK105 has a size of 85 nm and exhibits drug loading of 23%, and NC-6004 has a size of 20 nm, and loading capacity of 39%. Genexol-PM and NK105 particles carry paclitaxel, which is physically entrapped into both micelles, while NK-6004 particles carry a different drug (cisplatin) via coordinate bonding<sup>139</sup>. Drug release rates depend on drug loading, particle degradation and diffusivity of the drug molecules through the particle. For stimuli-responsive nanoparticles release rates will also depend on the intensity and efficiency of the stimulus. In any case, the ideal condition is for the nanoparticle to allow release of the drug only when it enters into the tumor tissue<sup>61</sup>.

## Design strategies to optimize delivery

A summary of the design guidelines described in the previous sections is presented in Table 3. Along with this information, which deals with the delivery aspect, we need also to take into account the drug loading and release rate of the nanoparticle as well as its, targeting capability (Figure 4). As this review focuses on the optimal delivery of nanoparticles, we propose three different design strategies.

### Small size nanoparticles

Nanoparticles with neutral charge and a size range of 12–50 nm would be ideal as far as transport is concerned. Such particles should have long circulation times and effective transvascular and interstitial transport. Therefore, they will distribute homogeneously and in larger amounts in the tumor interstitial space, which will also increase their intracellular delivery. From formulations currently in clinical use, micellar polymeric particles (i.e., NC-6004, NC-4016, NC-6300, and Genexol PM) as well as Abraxane and CRLX101 reside within this range. Liposomal formulations usually have a larger size in the range of 100 nm (e.g. Doxil, MM-398, TIL, VIL, Thermodox). Furthermore, increased sophistication to incorporate targeting ligands and/or controlled-release of the therapeutic load would increase the size of the particles. For instance, MCC-465 and SGT-53 are targeted liposomes with sizes > 100 nm, while BIND-014 and CALAA-01 are polymeric nanoparticles with sizes of 100 and 75 nm, respectively. Whether increased sophistication of nanomedicines overcomes delivery barriers posed by their large size will depend not only on the nanoparticle properties and drug-release kinetics but also on the tumor type.

### Elongated nanoparticle formulations

Elongated nanoparticles with neutral charge appear to have an advantage over spherical nanoparticles particularly due to their improved transport through the pores of the tumor

vessel wall and interstitial space<sup>55</sup>. In addition, elongated particles can have comparable blood circulation times with their spherical counterparts. Therefore, from the transport point of view there is a strong argument for the use of non-spherical particles such as nanorods or discoidal particles. Another parameter not mentioned thus far in our analysis is the rigidity of these particles. There is evidence that flexible particles of low elastic properties might have longer circulation times<sup>54,140,141</sup>. They are also expected to diffuse faster than rigid particles across the vessel wall and in the interstitial space due to their flexibility, and they will have weaker steric interactions with the structural components of the pores<sup>94</sup>. In addition, the advantageous transport properties of elongated particles would allow the use of larger formulations, which would increase their loading capacity. Finally, as far as the surface properties are concerned, it is a well-established strategy for the nanoparticles to be PEGylated in order to avoid reticuloendothelial clearance. As a result, particles usually have a neutral or near neutral charge, which can be also beneficial for interstitial transport into the tumor tissue.

### Multistage nanoparticle delivery systems

Fukumura et al<sup>142</sup> proposed a multistage system consisting of the primary particle that is loaded with smaller secondary particles, which in turn contain the therapeutic agent (Figure 4). From Table 3, we conclude that nano-carriers when injected into the blood have to be relatively large in order to ensure long circulation times, carry a large amount of secondary particles and therapeutic agents and avoid delivery to normal tissues. Additionally, the nano-carriers should be able to effectively cross the wall of tumor vessels. Therefore as far as transport is concerned, a particle size spanning from 12 to 60 nm would be ideal. However, if we account for their load capacity, particles as large as 100 nm might be also considered, particularly for hyper-permeable tumors. Once it enters the tumor interstitial space, the nano-carrier has to have efficient and homogeneous penetration into the tissue. This can be achieved by designing the delivery system such that the secondary particles are 5–10 nm in diameter. Finally, therapeutic agents carried by the secondary particles should be released to reach the cancer cells. Adding one more stage to the conventional nanoparticles might improve the distribution of the drug into the tumor and enhance the efficacy of the treatment. With the use of mathematical modeling, we found the benefit of multistage systems to be more pronounced for high binding affinities between drug molecules and tumor components<sup>131</sup>; however, this prediction needs to be tested experimentally.

Release of secondary particles inside the tumor can be achieved by making the particles responsive to the properties of the microenvironment. pH-responsive nanoparticles aim at utilizing the acidic microenvironment of many tumors. However, the decrease in pH is relatively small and occurs in a distance of several hundreds of micro-meters from the blood vessels<sup>143</sup>. Therefore, the particles need to be small enough to be able to diffuse into the acidic regions. Another approach that seems to be promising is the multistage particles whose size decreases in response to activated enzymes (MMPs) that are abundant in the microenvironment of many tumors or by hydrolysis<sup>142,144</sup>. An advantage of enzyme responsive systems is that MMPs (e.g., MMP-2 and MMP-9) are involved in tumor angiogenesis and cancer cell invasion and metastasis. Degradation of interstitial collagen by MMPs creates spaces for new vessels and movement of cells. Levels of MMP-2 and MMP-9

are high in perivascular regions and at the tumor margin where high vascular densities are observed and these are also the regions where nanoparticles are most likely to extravasate. MMPs are present in lower amounts in the blood plasma and in normal tissues, however, and thus, the kinetics of nanoparticle degradation must be carefully adjusted so that the system is responsive only in the tumor microenvironment.

## Closing remarks

In our analysis we focused on the effect of the physical properties of nanoparticles and we considered for passive delivery through the EPR effect. Stimuli responsive nanoparticles exist that respond to an internal stimulus of the tumor microenvironment such as pH, temperature, enzyme activity, Redox or an external source and particularly to a magnetic field, ultrasound, heat or light. The stimulus is used either to increase the concentration of the nanoparticles in the tumor site or to locally activate the particles in order to release the drug<sup>115,116</sup>. Furthermore, nanoparticles targeting cancer cells and use of tumor penetration peptides are other strategies that have the potential to increase specificity and efficacy of drug delivery systems.

Delivery of nanomedicines to solid tumors depends both on the tumor microenvironment and the properties of the nanoparticle formulations. Our analysis was focused on the nanoparticle side and provided general guidelines for optimal design. These design guidelines can be further specified if one accounts for the particular characteristics of tumor types, such as the permeability of the tumor vessels and the degree of tumor perfusion, as well as the density and composition of the tumor extracellular matrix<sup>1,3,8</sup>. Tumor blood vessels can be divided into hyper-permeable (e.g. some breast carcinomas) or moderately permeable (e.g. pancreatic neuroendocrine tumors), well perfused with functional blood vessels (e.g. glioblastomas or liver cancers) or hypo-perfused with abundant dysfunctional vessels (e.g., pancreatic, breast, colon adenocarcinomas and sarcomas). Also, there are highly desmoplastic tumors, rich in collagen and hyaluronic acid (e.g. fibrosarcomas, soft tissue sarcomas, pancreatic cancers) and others that have a moderate desmoplastic reaction (e.g., liver cancers). These parameters of the tumor microenvironment affect the design of nanoparticles and can explain why nano-therapy might have different response among tumor types. Treatments to modify the tumor microenvironment in order to make the tumor more accessible to nanomedicines are emerging and need to be exploited for improved outcomes<sup>3,17,90,145-149</sup>.

## Acknowledgments

This work was supported by the European Commission, Marie-Curie Reintegration grant (No. PIRG08-GA-2010-276894) to TS, the National Cancer Institute (P01-CA080124, R01-CA126642, R01-CA115767, R01-CA096915, R01-CA085140, R01-CA098706, Federal Share Income Grant), and a DoD Breast Cancer Research Innovator award (W81XWH-10-1-0016) to RKJ.

The manuscript is based on the reviews: Jain RK and Stylianopoulos T, *Nat Rev Clin Oncol*, 7, 653-664, 2010, and Chauhan VP and Jain RK, *Nat Mater*, 11, 958-962, 2013.

## References

1. Jain RK, Stylianopoulos T. Delivering nanomedicine to solid tumors. *Nat Rev Clin Oncol*. 2010; 7:653–64. [PubMed: 20838415]
2. Prabhakar U, Maeda H, Jain RK, Sevick-Muraca EM, Zamboni W, Farokhzad OC, et al. Challenges and Key Considerations of the Enhanced Permeability and Retention Effect for Nanomedicine Drug Delivery in Oncology. *Cancer Res*. 2013; 73:2412–7. [PubMed: 23423979]
3. Chauhan VP, Jain RK. Strategies for advancing cancer nanomedicine. *Nat Mater*. 2013; 12:958–62. [PubMed: 24150413]
4. Gerlowski LE, Jain RK. Microvascular permeability of normal and neoplastic tissues. *Microvasc Res*. 1986; 31:288–305. [PubMed: 2423854]
5. Matsumura Y, Maeda H. A new concept for macromolecular therapeutics in cancer chemotherapy: mechanism of tumoritropic accumulation of proteins and the antitumor agent Smancs. *Cancer Res*. 1986; 46:6387–92. [PubMed: 2946403]
6. Jain RK. Barriers to drug delivery in solid tumors. *Sci Am*. 1994; 271:58–65. [PubMed: 8066425]
7. Jain RK. Delivery of molecular and cellular medicine to solid tumors. *Adv Drug Deliv Rev*. 2001; 46:149–68. [PubMed: 11259838]
8. Chauhan VP, Stylianopoulos T, Boucher Y, Jain RK. Delivery of molecular and nanomedicine to tumors: Transport barriers and strategies. *Annual Reviews Chemical and Biomolecular Engineering*. 2011; 2:281–98.
9. Netti PA, Roberge S, Boucher Y, Baxter LT, Jain RK. Effect of transvascular fluid exchange on pressure-flow relationship in tumors: a proposed mechanism for tumor blood flow heterogeneity. *Microvasc Res*. 1996; 52:27–46. [PubMed: 8812751]
10. Stylianopoulos T, Jain RK. Combining two strategies to improve perfusion and drug delivery in solid tumors. *Proc Natl Acad Sci U S A*. 2013; 110:18632–7. [PubMed: 24167277]
11. Jain RK, Martin JD, Stylianopoulos T. The role of mechanical forces in tumor progression and therapy. *Annu Rev Biomed Eng*. 2014; 16:321–46. [PubMed: 25014786]
12. Jain RK, Baxter LT. Mechanisms of heterogeneous distribution of monoclonal antibodies and other macromolecules in tumors: significance of elevated interstitial pressure. *Cancer Res*. 1988; 48:7022–32. [PubMed: 3191477]
13. Boucher Y, Baxter LT, Jain RK. Interstitial pressure gradients in tissue-isolated and subcutaneous tumors: implications for therapy. *Cancer Res*. 1990; 50:4478–84. [PubMed: 2369726]
14. Boucher Y, Jain RK. Microvascular pressure is the principal driving force for interstitial hypertension in solid tumors: implications for vascular collapse. *Cancer Res*. 1992; 52:5110–4. [PubMed: 1516068]
15. Nugent LJ, Jain RK. Extravascular diffusion in normal and neoplastic tissues. *Cancer Res*. 1984; 44:238–44. [PubMed: 6197161]
16. Cabral H, Matsumoto Y, Mizuno K, Chen Q, Murakami M, Kimura M, et al. Accumulation of sub-100 nm polymeric micelles in poorly permeable tumours depends on size. *Nat Nanotechnol*. 2011; 6:815–23. [PubMed: 22020122]
17. Chauhan VP, Stylianopoulos T, Martin JD, Popovic Z, Chen O, Kamoun WS, et al. Normalization of tumour blood vessels improves the delivery of nanomedicines in a size-dependent manner. *Nat Nanotechnol*. 2012; 7:383–388. [PubMed: 22484912]
18. Stylianopoulos T. EPR-effect: utilizing size-dependent nanoparticle delivery to solid tumors. *Ther Deliv*. 2013; 4:421–3. [PubMed: 23557281]
19. Barenholz Y. Doxil(R)--the first FDA-approved nano-drug: lessons learned. *J Control Release*. 2012; 160:117–34. [PubMed: 22484195]
20. Bourzac K. Nanotechnology: Carrying drugs. *Nature*. 2012; 491:S58–60. [PubMed: 23320289]
21. Sheridan C. Proof of concept for next-generation nanoparticle drugs in humans. *Nat Biotechnol*. 2012; 30:471–3. [PubMed: 22678364]
22. Venditto VJ, Szoka FC Jr. Cancer nanomedicines: so many papers and so few drugs! *Adv. Drug Deliv Rev*. 2013; 65:80–8.

23. Dawidczyk CM, Russell LM, Searson PC. Nanomedicines for cancer therapy: state-of-the-art and limitations to pre-clinical studies that hinder future developments. *Front Chem.* 2014; 2:69. [PubMed: 25202689]
24. Bertrand N, Wu J, Xu X, Kamaly N, Farokhzad OC. Cancer nanotechnology: the impact of passive and active targeting in the era of modern cancer biology. *Adv Drug Deliv Rev.* 2014; 66:2–25. [PubMed: 24270007]
25. Northfelt DW, Dezube BJ, Thommes JA, Miller BJ, Fischl MA, Friedman-Kien A, et al. Pegylated-liposomal doxorubicin versus doxorubicin, bleomycin, and vincristine in the treatment of AIDS-related Kaposi's sarcoma: results of a randomized phase III clinical trial. *J Clin Oncol.* 1998; 16:2445–51. [PubMed: 9667262]
26. Gordon AN, Fleagle JT, Guthrie D, Parkin DE, Gore ME, Lacave AJ. Recurrent epithelial ovarian carcinoma: a randomized phase III study of pegylated liposomal doxorubicin versus topotecan. *J Clin Oncol.* 2001; 19:3312–22. [PubMed: 11454878]
27. O'Brien ME, Wigler N, Inbar M, Rosso R, Grischke E, Santoro A, et al. Reduced cardiotoxicity and comparable efficacy in a phase III trial of pegylated liposomal doxorubicin HCl (CAELYX/Doxil) versus conventional doxorubicin for first-line treatment of metastatic breast cancer. *Ann Oncol.* 2004; 15:440–9. [PubMed: 14998846]
28. Gill PS, Wernz J, Scadden DT, Cohen P, Mukwaya GM, von Roenn JH, et al. Randomized phase III trial of liposomal daunorubicin versus doxorubicin, bleomycin, and vincristine in AIDS-related Kaposi's sarcoma. *J Clin Oncol.* 1996; 14:2353–64. [PubMed: 8708728]
29. Batist G, Ramakrishnan G, Rao CS, Chandrasekharan A, Gutheil J, Guthrie T, et al. Reduced cardiotoxicity and preserved antitumor efficacy of liposome-encapsulated doxorubicin and cyclophosphamide compared with conventional doxorubicin and cyclophosphamide in a randomized, multicenter trial of metastatic breast cancer. *J Clin Oncol.* 2001; 19:1444–54. [PubMed: 11230490]
30. Gradishar WJ, Tjulandin S, Davidson N, Shaw H, Desai N, Bhar P, et al. Phase III trial of nanoparticle albumin-bound paclitaxel compared with polyethylated castor oil-based paclitaxel in women with breast cancer. *J Clin Oncol.* 2005; 23:7794–803. [PubMed: 16172456]
31. Von Hoff DD, Ervin T, Arena FP, Chiorean EG, Infante J, Moore M, et al. Increased survival in pancreatic cancer with nab-paclitaxel plus gemcitabine. *N Engl J Med.* 2013; 369:1691–703. [PubMed: 24131140]
32. Qiang C, Qizhong Z, Jian L, Liqing L, Wenhua Z, Yajie W. Multi-center prospective randomized trial on paclitaxel liposome and traditional taxol in the treatment of breast cancer and non-small-cell lung cancer. *Chin J Oncol.* 2003; 25:190–2.
33. Koudelka S, Turanek J. Liposomal paclitaxel formulations. *J Control Release.* 2012; 163:322–34. [PubMed: 22989535]
34. Lee KS, Chung HC, Im SA, Park YH, Kim CS, Kim SB, et al. Multicenter phase II trial of Genexol-PM, a Cremophor-free, polymeric micelle formulation of paclitaxel, in patients with metastatic breast cancer. *Breast Cancer Res Treat.* 2008; 108:241–50. [PubMed: 17476588]
35. Chen LT, Von Hoff DD, Li CP, Wang-Gillam A, Bodoky G, Dean A, et al. Expanded analyses of napoli-1: Phase 3 study of MM-398 (nal-IRI), with or without 5-fluorouracil and leucovorin, versus 5-fluorouracil and leucovorin, in metastatic pancreatic cancer (mPAC) previously treated with gemcitabine-based therapy. *J Clin Oncol.* 2015; 33(suppl 3):abstr 234.
36. Jain MM, Patil S, Pathak AB, Deshmukh CD, Bhatt N, Babu KG, et al. The efficacy and safety of paclitaxel injection concentrate for nano-dispersion (PICN) at two different doses versus paclitaxel albumin-stabilized nanoparticle formulation in subjects with metastatic breast cancer (MBC). *J Clin Oncol.* 2014; 32(suppl):abstr 1069.
37. Akhter S, Ahmad I, Ahmad MZ, Ramazani F, Singh A, Rahman Z, et al. Nanomedicines as cancer therapeutics: current status. *Curr Cancer Drug Targets.* 2013; 13:362–78. [PubMed: 23517593]
38. Svenson S. What nanomedicine in the clinic right now really forms nanoparticles? *Wiley Interdiscip. Rev Nanomed Nanobiotechnol.* 2014; 6:125–35.
39. Matsumura Y, Gotoh M, Muro K, Yamada Y, Shirao K, Shimada Y, et al. Phase I and pharmacokinetic study of MCC-465, a doxorubicin (DXR) encapsulated in PEG immunoliposome, in patients with metastatic stomach cancer. *Ann Oncol.* 2004; 15:517–25. [PubMed: 14998859]

40. Senzer N, Nemunaitis J, Nemunaitis D, Bedell C, Edelman G, Barve M, et al. Phase I study of a systemically delivered p53 nanoparticle in advanced solid tumors. *Mol Ther*. 2013; 21:1096–103. [PubMed: 23609015]
41. Hrkach J, Von Hoff D, Mukkaram Ali M, Andrianova E, Auer J, Campbell T, et al. Preclinical development and clinical translation of a PSMA-targeted docetaxel nanoparticle with a differentiated pharmacological profile. *Sci Transl Med*. 2012; 4:128ra39.
42. Davis ME. The first targeted delivery of siRNA in humans via a self-assembling, cyclodextrin polymer-based nanoparticle: from concept to clinic. *Mol Pharm*. 2009; 6:659–68. [PubMed: 19267452]
43. Davis ME, Zuckerman JE, Choi CH, Seligson D, Tolcher A, Alabi CA, et al. Evidence of RNAi in humans from systemically administered siRNA via targeted nanoparticles. *Nature*. 2010; 464:1067–70. [PubMed: 20305636]
44. Roy AC, Park SR, Cunningham D, Kang YK, Chao Y, Chen LT, et al. A randomized phase II study of PEP02 (MM-398), irinotecan or docetaxel as a second-line therapy in patients with locally advanced or metastatic gastric or gastro-oesophageal junction adenocarcinoma. *Ann Oncol*. 2013; 24:1567–73. [PubMed: 23406728]
45. Zuckerman JE, Gritli I, Tolcher A, Heidel JD, Lim D, Morgan R, et al. Correlating animal and human phase Ia/Ib clinical data with CALAA-01, a targeted, polymer-based nanoparticle containing siRNA. *Proc Natl Acad Sci US A*. 2014; 111:11449–54.
46. Sarin H. Physiologic upper limits of pore size of different blood capillary types and another perspective on the dual pore theory of microvascular permeability. *J Angiogenes Res*. 2010; 2:14. [PubMed: 20701757]
47. Longmire M, Choyke PL, Kobayashi H. Clearance properties of nano-sized particles and molecules as imaging agents: considerations and caveats. *Nanomedicine (Lond)*. 2008; 3:703–17. [PubMed: 18817471]
48. Choi HS, Liu W, Misra P, Tanaka E, Zimmer JP, Itty Ipe B, et al. Renal clearance of quantum dots. *Nat Biotechnol*. 2007; 25:1165–70. [PubMed: 17891134]
49. Choi HS, Liu W, Liu F, Nasr K, Misra P, Bawendi MG, et al. Design considerations for tumour-targeted nanoparticles. *Nat Nanotechnol*. 2010; 5:42–7. [PubMed: 19893516]
50. Zamboni WC, Torchilin V, Patri AK, Hrkach J, Stern S, Lee R, et al. Best practices in cancer nanotechnology: perspective from NCI nanotechnology alliance. *Clin Cancer Res*. 2012; 18:3229–41. [PubMed: 22669131]
51. Perrault SD, Walkey C, Jennings T, Fischer HC, Chan WC. Mediating tumor targeting efficiency of nanoparticles through design. *Nano Lett*. 2009; 9:1909–15. [PubMed: 19344179]
52. Popovic Z, Liu W, Chauhan VP, Lee J, Wong C, Greytak AB, et al. A nanoparticle size series for in vivo fluorescence imaging. *Angew Chem Int Ed Engl*. 2010; 49:8649–52. [PubMed: 20886481]
53. Singh R, Pantarotto D, Lacerda L, Pastorin G, Klumpp C, Prato M, et al. Tissue biodistribution and blood clearance rates of intravenously administered carbon nanotube radiotracers. *Proc Natl Acad Sci U S A*. 2006; 103:3357–62. [PubMed: 16492781]
54. Geng Y, Dalhaimer P, Cai S, Tsai R, Tewari M, Minko T, et al. Shape effects of filaments versus spherical particles in flow and drug delivery. *Nat Nanotechnol*. 2007; 2:249–55. [PubMed: 18654271]
55. Chauhan VP, Popovic Z, Chen O, Cui J, Fukumura D, Bawendi MG, et al. Fluorescent nanorods and nanospheres for real-time in vivo probing of nanoparticle shape-dependent tumor penetration. *Angew Chem Int Ed Engl*. 2011; 50:11417–11420. [PubMed: 22113800]
56. Peer D, Karp JM, Hong S, Farokhzad OC, Margalit R, Langer R. Nanocarriers as an emerging platform for cancer therapy. *Nat Nanotechnol*. 2007; 2:751–60. [PubMed: 18654426]
57. Klibanov AL, Maruyama K, Torchilin VP, Huang L. Amphipathic polyethyleneglycols effectively prolong the circulation time of liposomes. *FEBS Lett*. 1990; 268:235–7. [PubMed: 2384160]
58. Papahadjopoulos D, Allen TM, Gabizon A, Mayhew E, Matthay K, Huang SK, et al. Sterically stabilized liposomes: improvements in pharmacokinetics and antitumor therapeutic efficacy. *Proc Natl Acad Sci US A*. 1991; 88:11460–4.
59. Gref R, Luck M, Quellec P, Marchand M, Dellacherie E, Harnisch S, et al. ‘Stealth’ corona-core nanoparticles surface modified by polyethylene glycol (PEG): influences of the corona (PEG chain



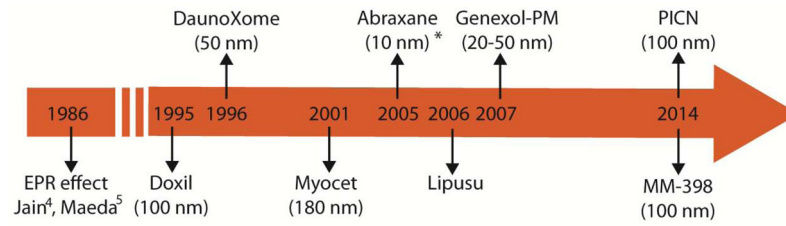
- length and surface density) and of the core composition on phagocytic uptake and plasma protein adsorption. *Colloids Surf B Biointerfaces*. 2000; 18:301–13. [PubMed: 10915952]
60. Perry JL, Reuter KG, Kai MP, Herlihy KP, Jones SW, Luft JC, et al. PEGylated PRINT nanoparticles: the impact of PEG density on protein binding, macrophage association, biodistribution, and pharmacokinetics. *Nano Lett*. 2012; 12:5304–10. [PubMed: 22920324]
61. Perry JL, Kai MP, Reuter KG, Bowerman C, Christopher Luft J, DeSimone JM. Calibration-quality cancer nanotherapeutics. *Cancer Treat Res*. 2015; 166:275–91. [PubMed: 25895873]
62. Garcia I, Marradi M, Penades S. Glyconanoparticles: multifunctional nanomaterials for biomedical applications. *Nanomedicine (Lond)*. 2010; 5:777–92. [PubMed: 20662648]
63. Pombo Garcia K, Zarschler K, Barbaro L, Barreto JA, O'Malley W, Spiccia L, et al. Zwitterionic-coated “stealth” nanoparticles for biomedical applications: recent advances in countering biomolecular corona formation and uptake by the mononuclear phagocyte system. *Small*. 2014; 10:2516–29. [PubMed: 24687857]
64. Hobbs SK, Monsky WL, Yuan F, Roberts WG, Griffith L, Torchilin VP, et al. Regulation of transport pathways in tumor vessels: role of tumor type and microenvironment. *Proc Natl Acad Sci U S A*. 1998; 95:4607–12. [PubMed: 9539785]
65. Boucher Y, Kirkwood JM, Opacic D, Desantis M, Jain RK. Interstitial hypertension in superficial metastatic melanomas in humans. *Cancer Res*. 1991; 51:6691–4. [PubMed: 1742743]
66. Less JR, Posner MC, Boucher Y, Borochovitz D, Wolmark N, Jain RK. Interstitial hypertension in human breast and colorectal tumors. *Cancer Res*. 1992; 52:6371–4. [PubMed: 1423283]
67. Yuan F, Salehi HA, Boucher Y, Vasthare US, Tuma RF, Jain RK. Vascular permeability and microcirculation of gliomas and mammary carcinomas transplanted in rat and mouse cranial windows. *Cancer Res*. 1994; 54:4564–8. [PubMed: 8062241]
68. Wiig H, Swartz MA. Interstitial fluid and lymph formation and transport: physiological regulation and roles in inflammation and cancer. *Physiol Rev*. 2012; 92:1005–60. [PubMed: 22811424]
69. Stylianopoulos T, Soteriou K, Fukumura D, Jain RK. Cationic nanoparticles have superior transvascular flux into solid tumors: Insights from a mathematical model. *Ann Biomed Eng*. 2013; 41(1):68–77. [PubMed: 22855118]
70. Yue J, Liu S, Xie Z, Xing Y, Jing X. Size-dependent biodistribution and antitumor efficacy of polymer micelle drug delivery systems. *J Mater Chem B*. 2013; 1:4273–4280.
71. Jacobetz MA, Chan DS, Neesse A, Bapiro TE, Cook N, Frese KK, et al. Hyaluronan impairs vascular function and drug delivery in a mouse model of pancreatic cancer. *Gut*. 2012; 62:112–20. [PubMed: 22466618]
72. Dotan E, Starodub A, Berlin J, Lieu CH, Guarino MJ, Marshall J, et al. A new anti-CEA-SN-38 antibody-drug conjugate (ADC), IMMU-130, is active in controlling metastatic colorectal cancer (mCRC) in patients (pts) refractory or relapsing after irinotecan-containing chemotherapies: Initial results of a phase I/II study. *ASCO Annual Meeting*. 2015:Abstr 2505.
73. Matsumura Y. Cancer stromal targeting (CAST) therapy. *Adv Drug Deliv Rev*. 2012; 64:710–9. [PubMed: 22212902]
74. Dellian M, Yuan F, Trubetsky VS, Torchilin VP, Jain RK. Vascular permeability in a human tumour xenograft: molecular charge dependence. *Br J Cancer*. 2000; 82:1513–8. [PubMed: 10789717]
75. Schmitt-Sody M, Strieth S, Krasnici S, Sauer B, Schulze B, Teifel M, et al. Neovascular targeting therapy: paclitaxel encapsulated in cationic liposomes improves antitumoral efficacy. *Clin Cancer Res*. 2003; 9:2335–41. [PubMed: 12796403]
76. Krasnici S, Werner A, Eichhorn ME, Schmitt-Sody M, Pahernik SA, Sauer B, et al. Effect of the surface charge of liposomes on their uptake by angiogenic tumor vessels. *Int J Cancer*. 2003; 105:561–7. [PubMed: 12712451]
77. Campbell RB, Fukumura D, Brown EB, Mazzola LM, Izumi Y, Jain RK, et al. Cationic charge determines the distribution of liposomes between the vascular and extravascular compartments of tumors. *Cancer Res*. 2002; 62:6831–6. [PubMed: 12460895]
78. Yim H, Park SJ, Bae YH, Na K. Biodegradable cationic nanoparticles loaded with an anticancer drug for deep penetration of heterogeneous tumours. *Biomaterials*. 2013; 34:7674–82. [PubMed: 23871541]

79. Han HS, Martin JD, Lee J, Harris DK, Fukumura D, Jain RK, et al. Spatial charge configuration regulates nanoparticle transport and binding behavior in vivo. *Angew Chem Int Ed Engl.* 2013; 52:1414–9. [PubMed: 23255143]
80. Zhou Z, Ma X, Jin E, Tang J, Sui M, Shen Y, et al. Linear-dendritic drug conjugates forming long-circulating nanorods for cancer-drug delivery. *Biomaterials.* 2013; 34:5722–35. [PubMed: 23639529]
81. Gentile F, Chiappini C, Fine D, Bhavane RC, Peluccio MS, Cheng MM, et al. The effect of shape on the margination dynamics of non-neutrally buoyant particles in two-dimensional shear flows. *J Biomech.* 2008; 41:2312–8. [PubMed: 18571181]
82. Smith BR, Kempen P, Bouley D, Xu A, Liu Z, Melosh N, et al. Shape matters: intravital microscopy reveals surprising geometrical dependence for nanoparticles in tumor models of extravasation. *Nano Lett.* 2012; 12:3369–77. [PubMed: 22650417]
83. Pluen A, Boucher Y, Ramanujan S, McKee TD, Gohongi T, di Tomaso E, et al. Role of tumor-host interactions in interstitial diffusion of macromolecules: cranial vs. subcutaneous tumors. *Proc Natl Acad Sci U S A.* 2001; 98:4628–33. [PubMed: 11274375]
84. Stylianopoulos T, Poh MZ, Insin N, Bawendi MG, Fukumura D, Munn LL, et al. Diffusion of particles in the extracellular matrix: The effect of repulsive electrostatic interactions. *Biophys J.* 2010; 99:1342–9. [PubMed: 20816045]
85. Stylianopoulos T, Diop-Frimpong B, Munn LL, Jain RK. Diffusion anisotropy in collagen gels and tumors: The effect of fiber network orientation. *Biophys J.* 2010; 99:3119–28. [PubMed: 21081058]
86. Baxter LT, Jain RK. Transport of fluid and macromolecules in tumors. I Role of interstitial pressure and convection. *Microvasc Res.* 1989; 37:77–104. [PubMed: 2646512]
87. Jain RK, Tong RT, Munn LL. Effect of vascular normalization by antiangiogenic therapy on interstitial hypertension, peritumor edema, and lymphatic metastasis: insights from a mathematical model. *Cancer Res.* 2007; 67:2729–35. [PubMed: 17363594]
88. Ramanujan S, Pluen A, McKee TD, Brown EB, Boucher Y, Jain RK. Diffusion and convection in collagen gels: implications for transport in the tumor interstitium. *Biophys J.* 2002; 83:1650–60. [PubMed: 12202388]
89. McKee TD, Grandi P, Mok W, Alexandrakis G, Insin N, Zimmer JP, et al. Degradation of fibrillar collagen in a human melanoma xenograft improves the efficacy of an oncolytic herpes simplex virus vector. *Cancer Res.* 2006; 66:2509–13. [PubMed: 16510565]
90. Diop-Frimpong B, Chauhan VP, Krane S, Boucher Y, Jain RK. Losartan inhibits collagen I synthesis and improves the distribution and efficacy of nanotherapeutics in tumors. *Proc Natl Acad Sci U S A.* 2011; 108:2909–14. [PubMed: 21282607]
91. Huo S, Ma H, Huang K, Liu J, Wei T, Jin S, et al. Superior penetration and retention behavior of 50 nm gold nanoparticles in tumors. *Cancer Res.* 2013; 73:319–30. [PubMed: 23074284]
92. Yuan F, Leunig M, Huang SK, Berk DA, Papahadjopoulos D, Jain RK. Microvascular permeability and interstitial penetration of sterically stabilized (stealth) liposomes in a human tumor xenograft. *Cancer Res.* 1994; 54:3352–6. [PubMed: 8012948]
93. Lieleg O, Baumgartel RM, Bausch AR. Selective filtering of particles by the extracellular matrix: an electrostatic bandpass. *Biophys J.* 2009; 97:1569–77. [PubMed: 19751661]
94. Pluen A, Netti PA, Jain RK, Berk DA. Diffusion of macromolecules in agarose gels: comparison of linear and globular configurations. *Biophys J.* 1999; 77:542–52. [PubMed: 10388779]
95. Rejman J, Oberle V, Zuhorn IS, Hoekstra D. Size-dependent internalization of particles via the pathways of clathrin- and caveolae-mediated endocytosis. *Biochem J.* 2004; 377:159–69. [PubMed: 14505488]
96. Gao H, Shi W, Freund LB. Mechanics of receptor-mediated endocytosis. *Proc Natl Acad Sci U S A.* 2005; 102:9469–74. [PubMed: 15972807]
97. Foged C, Brodin B, Frokjaer S, Sundblad A. Particle size and surface charge affect particle uptake by human dendritic cells in an in vitro model. *Int J Pharm.* 2005; 298:315–22. [PubMed: 15961266]
98. Chithrani BD, Ghazani AA, Chan WC. Determining the size and shape dependence of gold nanoparticle uptake into mammalian cells. *Nano Lett.* 2006; 6:662–8. [PubMed: 16608261]

99. Jiang W, Kim BY, Rutka JT, Chan WC. Nanoparticle-mediated cellular response is size-dependent. *Nat Nanotechnol.* 2008; 3:145–50. [PubMed: 18654486]
100. Rudolph C, Plank C, Lausier J, Schillinger U, Muller RH, Rosenecker J. Oligomers of the arginine-rich motif of the HIV-1 TAT protein are capable of transferring plasmid DNA into cells. *J Biol Chem.* 2003; 278:11411–8. [PubMed: 12519756]
101. Gratton SE, Ropp PA, Pohlhaus PD, Luft JC, Madden VJ, Napier ME, et al. The effect of particle design on cellular internalization pathways. *Proc Natl Acad Sci U S A.* 2008; 105:11613–8. [PubMed: 18697944]
102. Thorek DL, Tsourkas A. Size, charge and concentration dependent uptake of iron oxide particles by non-phagocytic cells. *Biomaterials.* 2008; 29:3583–90. [PubMed: 18533252]
103. Belting M. Heparan sulfate proteoglycan as a plasma membrane carrier. *Trends Biochem Sci.* 2003; 28:145–51. [PubMed: 12633994]
104. Harush-Frenkel O, Rozentur E, Benita S, Altschuler Y. Surface charge of nanoparticles determines their endocytic and transcytotic pathway in polarized MDCK cells. *Biomacromolecules.* 2008; 9:435–43. [PubMed: 18189360]
105. Huang X, Teng X, Chen D, Tang F, He J. The effect of the shape of mesoporous silica nanoparticles on cellular uptake and cell function. *Biomaterials.* 2010; 31:438–48. [PubMed: 19800115]
106. Champion JA, Mitragotri S. Role of target geometry in phagocytosis. *Proc Natl Acad Sci U S A.* 2006; 103:4930–4. [PubMed: 16549762]
107. Torchilin VP. Multifunctional, stimuli-sensitive nanoparticulate systems for drug delivery. *Nat Rev Drug Discov.* 2014; 13:813–27. [PubMed: 25287120]
108. Gianella A, Mieszawska AJ, Hoeben FJ, Janssen HM, Jarzyna PA, Cormode DP, et al. Synthesis and in vitro evaluation of a multifunctional and surface-switchable nanoemulsion platform. *Chem Commun(Camb).* 2013; 49:9392–4. [PubMed: 23877789]
109. McQuade C, Al Zaki A, Desai Y, Vido M, Sakhuja T, Cheng Z, et al. A Multifunctional NanoplatforM for Imaging, Radiotherapy, and the Prediction of Therapeutic Response. *Small.* 2015; 11:834–43. [PubMed: 25264301]
110. Das M, Duan W, Sahoo SK. Multifunctional nanoparticle-EpCAM aptamer bioconjugates: A paradigm for targeted drug delivery and imaging in cancer therapy. *Nanomedicine.* 2015; 11:379–89. [PubMed: 25240596]
111. Li J, Cai P, Shalviri A, Henderson JT, He C, Foltz WD, et al. A Multifunctional Polymeric Nanotheranostic System Delivers Doxorubicin and Imaging Agents across the Blood-Brain Barrier Targeting Brain Metastases of Breast Cancer. *ACS Nano.* 2014; 8:9925–40. [PubMed: 25307677]
112. Zhu L, Kate P, Torchilin VP. Matrix metalloprotease 2-responsive multifunctional liposomal nanocarrier for enhanced tumor targeting. *ACS Nano.* 2012; 6:3491–8. [PubMed: 22409425]
113. Zhou J, Patel TR, Fu M, Bertram JP, Saltzman WM. Octa-functional PLGA nanoparticles for targeted and efficient siRNA delivery to tumors. *Biomaterials.* 2012; 33:583–91. [PubMed: 22014944]
114. Park JH, von Maltzahn G, Zhang L, Derfus AM, Simberg D, Harris TJ, et al. Systematic surface engineering of magnetic nanoworms for in vivo tumor targeting. *Small.* 2009; 5:694–700. [PubMed: 19263431]
115. Zhu L, Torchilin VP. Stimulus-responsive nanopreparations for tumor targeting. *Integr Biol(Camb).* 2013; 5:96–107. [PubMed: 22869005]
116. Mura S, Nicolas J, Couvreur P. Stimuli-responsive nanocarriers for drug delivery. *Nat Mater.* 2013; 12:991–1003. [PubMed: 24150417]
117. Blum AP, Kammeyer JK, Rush AM, Callmann CE, Hahn ME, Gianneschi NC. Stimuli-responsive nanomaterials for biomedical applications. *J Am Chem Soc.* 2015; 137:2140–54. [PubMed: 25474531]
118. von Maltzahn G, Park JH, Agrawal A, Bandaru NK, Das SK, Sailor MJ, et al. Computationally guided photothermal tumor therapy using long-circulating gold nanorod antennas. *Cancer Res.* 2009; 69:3892–900. [PubMed: 19366797]

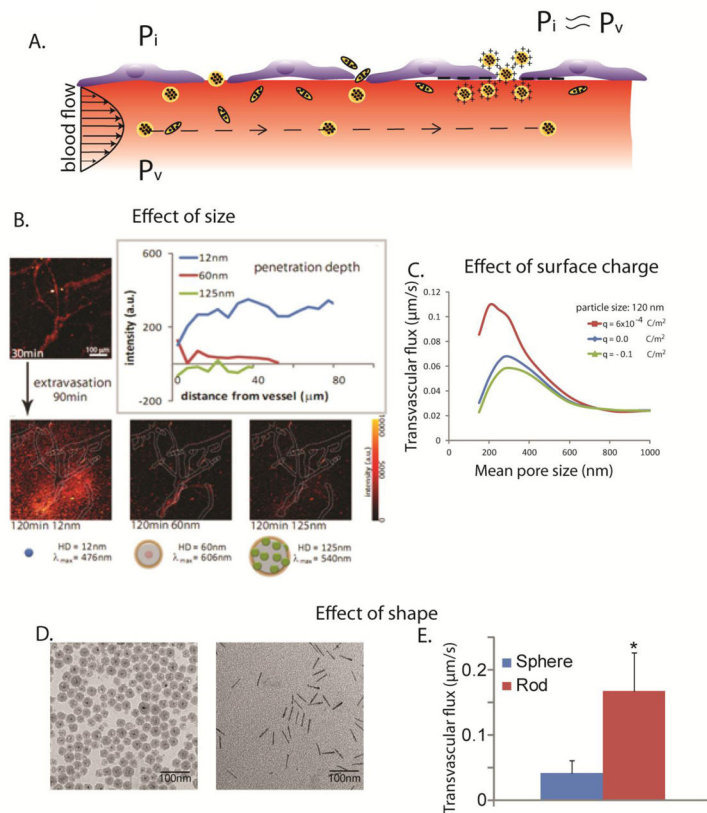
119. Fomina N, Sankaranarayanan J, Almutairi A. Photochemical mechanisms of light-triggered release from nanocarriers. *Adv Drug Deliv Rev.* 2012; 64:1005–20. [PubMed: 22386560]
120. Ruoslahti E. Peptides as targeting elements and tissue penetration devices for nanoparticles. *Adv Mater.* 2012; 24:3747–56. [PubMed: 22550056]
121. Akerman ME, Chan WC, Laakkonen P, Bhatia SN, Ruoslahti E. Nanocrystal targeting in vivo. *Proc Natl Acad Sci U S A.* 2002; 99:12617–21. [PubMed: 12235356]
122. Sugahara KN, Teesalu T, Karmali PP, Kotamraju VR, Agemy L, Girard OM, et al. Tissue-penetrating delivery of compounds and nanoparticles into tumors. *Cancer Cell.* 2009; 16:510–20. [PubMed: 19962669]
123. Karmali PP, Kotamraju VR, Kastantin M, Black M, Missirlis D, Tirrell M, et al. Targeting of albumin-embedded paclitaxel nanoparticles to tumors. *Nanomedicine.* 2009; 5:73–82. [PubMed: 18829396]
124. Sugahara KN, Teesalu T, Karmali PP, Kotamraju VR, Agemy L, Greenwald DR, et al. Coadministration of a tumor-penetrating peptide enhances the efficacy of cancer drugs. *Science.* 2010; 328:1031–35. [PubMed: 20378772]
125. Kinsella JM, Jimenez RE, Karmali PP, Rush AM, Kotamraju VR, Gianneschi NC, et al. X-ray computed tomography imaging of breast cancer by using targeted peptide-labeled bismuth sulfide nanoparticles. *Angew Chem Int Ed Engl.* 2011; 50:12308–11. [PubMed: 22028313]
126. Winer I, Wang S, Lee YE, Fan W, Gong Y, Burgos-Ojeda D, et al. F3-targeted cisplatin-hydrogel nanoparticles as an effective therapeutic that targets both murine and human ovarian tumor endothelial cells in vivo. *Cancer Res.* 2010; 70:8674–83. [PubMed: 20959470]
127. Minchinton AI, Tannock IF. Drug penetration in solid tumours. *Nat Rev Cancer.* 2006; 6:583–92. [PubMed: 16862189]
128. Fujimori K, Covell DG, Fletcher JE, Weinstein JN. A modeling analysis of monoclonal antibody percolation through tumors: a binding-site barrier. *J Nucl Med.* 1990; 31:1191–8. [PubMed: 2362198]
129. Baxter LT, Jain RK. Transport of fluid and macromolecules in tumors. IV A microscopic model of the perivascular distribution. *Microvasc Res.* 1991; 41:252–72. [PubMed: 2051960]
130. Schmidt MM, Wittrup KD. A modeling analysis of the effects of molecular size and binding affinity on tumor targeting. *Mol Cancer Ther.* 2009; 8:2861–71. [PubMed: 19825804]
131. Stylianopoulos T, Economides EA, Baish J, Fukumura D, Jain RK. Optimal design of cancer nanomedicines: Multi-stage nanoparticle delivery systems for the treatment of solid tumors. *Annals of Biomedical Engineering.* 2015; 10.1007/s10439-015-1276-9
132. Lammers T, Kiessling F, Hennink WE, Storm G. Drug targeting to tumors: principles, pitfalls and (pre-) clinical progress. *J Control Release.* 2012; 161:175–87. [PubMed: 21945285]
133. Cheng Z, Al Zaki A, Hui JZ, Muzykantov VR, Tsourkas A. Multifunctional nanoparticles: cost versus benefit of adding targeting and imaging capabilities. *Science.* 2012; 338:903–10. [PubMed: 23161990]
134. Verma S, Miles D, Gianni L, Krop IE, Welslau M, Baselga J, et al. Trastuzumab emtansine for HER2-positive advanced breast cancer. *N Engl J Med.* 2012; 367:1783–91. [PubMed: 23020162]
135. Pirolo KF, Chang EH. Does a targeting ligand influence nanoparticle tumor localization or uptake? *Trends Biotechnol.* 2008; 26:552–8. [PubMed: 18722682]
136. Lee H, Fonge H, Hoang B, Reilly RM, Allen C. The effects of particle size and molecular targeting on the intratumoral and subcellular distribution of polymeric nanoparticles. *Mol Pharm.* 2010; 7:1195–208. [PubMed: 20476759]
137. Sanson C, Schatz C, Le Meins JF, Soum A, Thevenot J, Garanger E, et al. A simple method to achieve high doxorubicin loading in biodegradable polymersomes. *J Control Release.* 2010; 147:428–35. [PubMed: 20692308]
138. Gong J, Huo M, Zhou J, Zhang Y, Peng X, Yu D, et al. Synthesis, characterization, drug-loading capacity and safety of novel octyl modified serum albumin micelles. *Int J Pharm.* 2009; 376:161–8. [PubMed: 19409461]
139. Gong J, Chen M, Zheng Y, Wang S, Wang Y. Polymeric micelles drug delivery system in oncology. *J Control Release.* 2012; 159:312–23. [PubMed: 22285551]

140. Merkel TJ, Jones SW, Herlihy KP, Kersey FR, Shields AR, Napier M, et al. Using mechanobiological mimicry of red blood cells to extend circulation times of hydrogel microparticles. *Proc Natl Acad Sci US A*. 2011; 108:586–91.
141. Agarwal R, Roy K. Intracellular delivery of polymeric nanocarriers: a matter of size, shape, charge, elasticity and surface composition. *Ther Deliv*. 2013; 4:705–23. [PubMed: 23738668]
142. Wong C, Stylianopoulos T, Cui J, Martin J, Chauhan VP, Jiang W, et al. Multistage nanoparticle delivery system for deep penetration into tumor tissue. *Proc Natl Acad Sci U S A*. 2011; 108:2426–31. [PubMed: 21245339]
143. Helmlinger G, Yuan F, Dellian M, Jain RK. Interstitial pH and pO<sub>2</sub> gradients in solid tumors in vivo: high-resolution measurements reveal a lack of correlation. *Nat Med*. 1997; 3:177–82. [PubMed: 9018236]
144. Stylianopoulos T, Wong C, Bawendi MG, Jain RK, Fukumura D. Multistage nanoparticles for improved delivery into tumor tissue. *Methods in Enzymology*. 2012; 508:109–30. [PubMed: 22449923]
145. Stylianopoulos T, Martin JD, Chauhan VP, Jain SR, Diop-Frimpong B, Bardeesy N, et al. Causes, consequences, and remedies for growth-induced solid stress in murine and human tumors. *Proc Natl Acad Sci US A*. 2012; 109:15101–8.
146. Provenzano PP, Cuevas C, Chang AE, Goel VK, Von Hoff DD, Hingorani SR. Enzymatic targeting of the stroma ablates physical barriers to treatment of pancreatic ductal adenocarcinoma. *Cancer Cell*. 2012; 21:418–29. [PubMed: 22439937]
147. Liu J, Liao S, Diop-Frimpong B, Chen W, Goel S, Naxerova K, et al. TGF- $\beta$  blockade improves the distribution and efficacy of therapeutics in breast carcinoma by normalizing the tumor stroma. *Proc Natl Acad Sci U S A*. 2012; 109:16618–23. [PubMed: 22996328]
148. Chauhan VP, Martin JD, Liu H, Lacorre DA, Jain SR, Kozin SV, et al. Angiotensin inhibition enhances drug delivery and potentiates chemotherapy by decompressing tumor blood vessels. *Nature Communications*. 2013; 410.1038/ncomms.3516
149. Chauhan VP, Boucher Y, Ferrone CR, Roberge S, Martin JD, Stylianopoulos T, et al. Compression of pancreatic tumor blood vessels by hyaluronan is caused by solid stress and not interstitial fluid pressure. *Cancer Cell*. 2014; 26:14–5. [PubMed: 25026209]

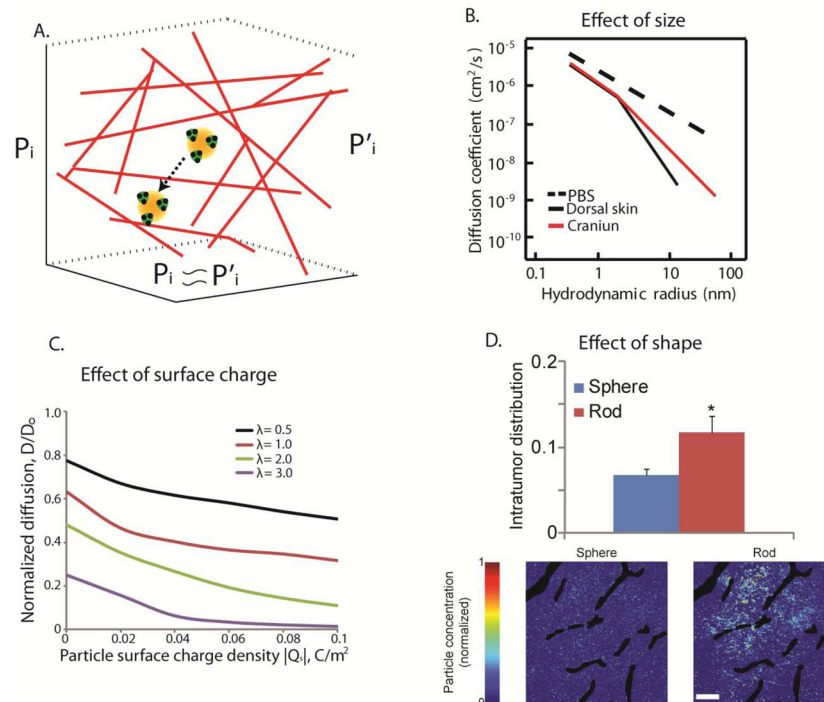


**Figure 1.**

Chronology of first clinical approvals of nanomedicines after the introduction of the EPR effect. Myocet is approved only in Europe and Canada, Lipusu in China, Genexol-PM in South Korea and PICN in India. The size of nanoparticles given in parenthesis is approximate. \*Abraxane becomes ~10 nm in size from ~130 nm following disintegration in the blood<sup>17</sup>. The size of Lipusu is not available.

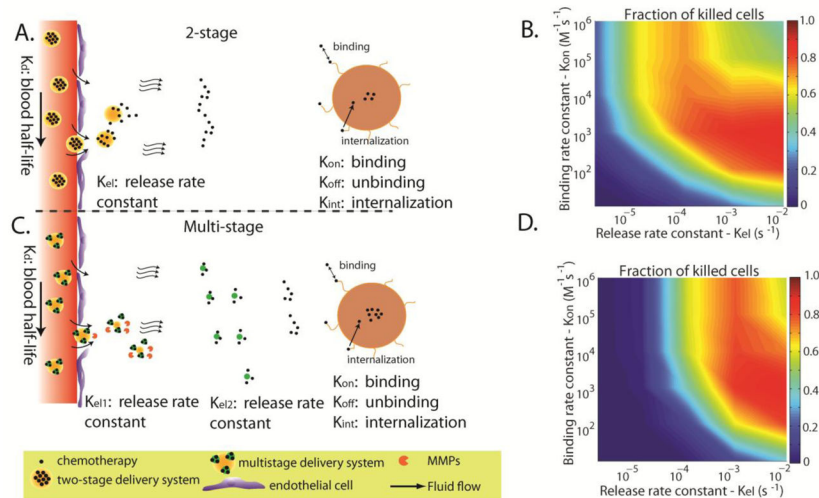
**Figure 2.**

Effect of particle physicochemical properties on transvascular transport. A.) Interstitial fluid pressure,  $P_i$ , in solid tumors is elevated and is approximately equal to microvascular pressure,  $P_v$ , which eliminates transvascular pressure gradients and renders diffusion the dominant mechanism of transport. Spherical particles move with the flow, while elongated particles rotate as they move and interact with the vessel wall. Cationic particles are concentrated near the vessel wall owing to electrostatic attractions. B.) Transvascular transport of nanoparticles is size-dependent, with small nanoparticles, less than 60 nm in diameter, able to effectively extravasate (adapted with permission from <sup>52</sup>). C.) Cationic nanoparticles have superior transvascular flux in solid tumors, with  $q$  [Coulomb/m<sup>2</sup>] being the surface charge density (simulation results obtained with permission from <sup>69</sup>) and D. and E.) Rods can more effectively extravasate into the tumor compared with spherical particles of the same hydrodynamic diameter. Asterisk denotes a statistically significant difference (obtained with permission from <sup>55</sup>).



**Figure 3.** Effect of particle physicochemical properties on interstitial transport. A.) Interstitial fluid pressure is often uniformly elevated rendering diffusion the main mechanism of interstitial transport within the pores of the collagen network in the tumor interstitial space (adapted with permission from <sup>85</sup>). B.) Size-dependent interstitial diffusivity as a function of the hydrodynamic radius for diffusion in PBS, the dorsal skin and the brain (with permission from <sup>83</sup>). C.) Simulation results for the effect of electrostatic repulsion on interstitial diffusivity. Normalized diffusion is the ratio of the diffusion coefficient in the tissue over the diffusion coefficient in water and  $\lambda$  is the ratio of particle radius divided by the fiber radius (with permission from <sup>69</sup>). D.) Effect of particle shape on the interstitial transport of nanoparticles. Intratumor distribution refers to the area of tumor sections occupied by the particles and the distribution of the spherical and rod-like particles in a tumor section (Bottom). Asterisk denotes a statistically significant difference (with permission from <sup>55</sup>).



**Figure 4.**

Effect of binding affinity and drug release rate on the efficacy of two-stage and multistage drug delivery systems. A.) Conventional, two-stage delivery systems are composed of the nano-carrier and the drug. The drug is released by the nano-carrier in a controlled fashion. B.) Optimization contour plot of the fraction of killed cells as a function of the binding affinity of the drug and the drug release rate. C.) Multi-stage drug delivery systems consist of an extra step in the delivery of nanomedicines to solid tumors including a primary nanoparticle, a secondary nanoparticle and the drug. D.) Optimization contour plot for a multi-stage delivery system (Adapted with permission from <sup>131</sup>).

**Table 1**

Nanoparticle formulations clinically approved for treatment of solid tumors. Indications, survival benefit and reduction in adverse effects (adapted and updated from Ref<sup>1</sup>).

<b>Drug</b>	<b>Indication</b>	<b>Survival benefit</b>	<b>Benefit on adverse effects</b>
Doxil/Caelyx (Pegylated liposomal doxorubicin)	HIV-related Kaposi's sarcoma	No statistically significant increase in overall survival (23 weeks) versus doxorubicin, bleomycin and vincristine treatment (22.3 weeks) for HIV-related Kaposi's sarcoma. <sup>25</sup>	Statistically significant decrease in nausea/vomiting, alopecia and peripheral neuropathy. <sup>25</sup>
	Metastatic ovarian cancer	Statistically significant increase in overall survival (108 weeks, $P = 0.008$ ) versus topotecan treatment (71.1 weeks) for platinum-sensitive patients with ovarian cancer. <sup>26</sup>	Statistically significant decrease in neutropenia, anemia, thrombocytopenia, leukopenia and alopecia. <sup>26</sup>
	Metastatic breast cancer	No statistically significant change in overall survival (84 weeks) versus conventional doxorubicin (88 weeks) for first-line breast cancer patients. <sup>27</sup>	Statistically significant decrease in cardiotoxicity, alopecia, nausea/vomiting, and neutropenia. <sup>27</sup>
DaunoXome (liposomal daunorubicin)	HIV-related Kaposi's sarcoma	No statistically significant change in overall survival (52.7 weeks) versus doxorubicin, bleomycin and vincristine treatment (48.9 weeks). <sup>28</sup>	Statistically significant decrease in alopecia and neuropathy. <sup>28</sup>
Myocet (liposomal doxorubicin)	Metastatic breast cancer	No statistically significant change in overall survival of Myocet and cyclophosphamide (49 months) versus doxorubicin and cyclophosphamide (48 months). <sup>29</sup>	Statistically significant decrease in cardiotoxicity and grade 4 neutropenia. <sup>29</sup>
Abraxane (albumin-bound paclitaxel)	Metastatic breast cancer	Statistically significant increase in overall survival (56.4 weeks, $P = 0.024$ ) versus polyethylated castor oil-based paclitaxel treatment (46.7 weeks) for second-line patients. <sup>30</sup>	Statistically significant decrease in neutropenia. No hypersensitivity reactions. <sup>30</sup>
	Pancreatic ductal adenocarcinoma	Statistically significant increase in overall survival (8.5 months, $P < 0.001$ ) of Abraxane plus gemcitabine versus gemcitabine alone (6.7 months). <sup>31</sup>	Proportion of patients with serious adverse events was similar in the two treatment groups. <sup>31</sup>
Lipusu (liposomal paclitaxel)	Breast and non- small-cell lung cancer	No statistically significant difference in efficacy vs conventional paclitaxel. <sup>32,33</sup>	Reduced hypersensitivity reactions. <sup>32,33</sup>
Genexol-PM (micelle of paclitaxel)	Metastatic breast cancer	Overall response rate 58.5% in a Phase II trial. <sup>34</sup>	Reduced hypersensitivity reactions. <sup>34</sup>

<b>Drug</b>	<b>Indication</b>	<b>Survival benefit</b>	<b>Benefit on adverse effects</b>
MM-398 (Liposomal formulation of irinotecan)	Pancreatic ductal adenocarcinoma	Statistically significant increase in overall survival (6.1 months, P<0.001) with MM-398 plus 5-fluorouracil and leucovorin (5-FU/LV) versus 5-FU/LV (4.2 months). <sup>35</sup>	Most frequent adverse effects compared to 5-FU/LV include neutropenia, fatigue, diarrhea and vomiting. <sup>35</sup>
PICN (Paclitaxel injection concentrate for nanodispersion)	Metastatic breast cancer	Not statistically significant difference in objective response rate compared to Abraxane. <sup>36</sup>	No hypersensitivity reactions. <sup>36</sup>

Author Manuscript

Author Manuscript

Author Manuscript

Author Manuscript

**Table 2**

Examples of nanoparticle formulations currently in clinical trials.

Formulation	Description	Size (nm)	In clinical trials for
Lipusu	Liposomal formulation of paclitaxel	Not available	Metastatic breast cancer (Phase IV, NCT02142790), advanced solid tumors (Phase IV, NCT01994031).
MCC-465	Targeted liposomal formulation of doxorubicin	143	Metastatic stomach cancer (Phase I/II in Japan).
SGT-53	Targeted liposomal formulation of p53 gene	115	Solid tumors (Phase I, NCT00470613), metastatic pancreatic cancer (Phase II, NCT02340117), refractory or recurrent solid tumors (Phase I, NCT02354547), recurrent glioblastoma (Phase II, NCT02354547).
PICN	Paclitaxel injection concentrate for nanodispersion	100	Metastatic or recurrent breast cancer (phase I, NCT02136927), solid tumors in advanced stages (Phase I, NCT01305512, NCT01304303).
MM-398	Liposomal formulation of irinotecan	100	Gastric or gastro-esophageal junction adenocarcinoma (Phase II <sup>44</sup> ), pediatric solid tumors (Phase I, NCT02013336), various breast cancers (Phase I, NCT01770353), high grade gliomas (Phase I, NCT02022644).
TIL	Liposomal formulation of topotecan	100	Small cell lung cancer, ovarian cancer, other advanced tumors (Phase I, NCT00765973).
VIL	Liposomal formulation of vinorelbine	100	Advanced solid tumors (Phase I, NCT00364676).
Thermodox	Heat-activated liposomal formulation of doxorubicin	100	Liver cancer (Phase III, NCT00617981, NCT02112656, Phase I, NCT02181075), breast cancer (Phase I/II, NCT00826085).
LiPlaCis	Liposomal formulation of cisplatin	Not available	Advanced or refractory solid tumors (Phase I, NCT01861496).
BIND-014	Targeted polymeric nanoparticle containing docetaxel	100	Prostate cancer (Phase II, NCT01812746, <sup>41</sup> ) and non-small cell lung cancer (Phase II, NCT01792479).
NK105	Micellar polymeric nanoparticle incorporating paclitaxel	85	Metastatic or recurrent breast cancer (Phase III, NCT01644890).
TKM- 080301	Liposomal formulation of PLK1 siRNA	80	Neuroendocrine tumors, Adrenocortical carcinoma (Phase I/II, NCT01262235).
Atu027	Liposomal formulation of PKN3 siRNA	Not Available	Advanced or metastatic pancreatic cancer (Phase I/II, NCT01808638).
CALAA-01	Targeted polymeric nanoparticle containing gene silencing RNA	75	Various cancers (Phase I <sup>45</sup> ).
NC-6300	Micellar polymeric nanoparticle incorporating epirubicin	40–80	Various cancers (Phase I, in Japan)
NC-4016	Micellar polymeric nanoparticle incorporating oxaliplatin	40	Advanced solid tumors or lymphomas (Phase I, NCT01999491).
CRLX101	Cyclodextrin-containing polymer conjugated to camptothecin	30–40	Recurrent non-small cell lung cancer (Phase II, NCT01803269), metastatic renal cell carcinoma (Phase II, NCT02187302), ovarian/tubal/peritoneal cancer (Phase II, NCT01652079, Phase I, NCT02389985), rectal cancer (Phase I/II, NCT02010567).
Genexol-PM	Micellar polymeric nanoparticle incorporating paclitaxel	20–50	Metastatic breast cancer (Phase II, NCT01784120), head and neck cancer (Phase II, NCT01689194).
NC-6004	Micellar polymeric nanoparticle incorporating cispatlin	20	Locally advanced or metastatic pancreatic cancer (Phase III, NCT02043288) and non-small cell lung cancer (Phase I/II, NCT02240238).

**Table 3**

Design considerations for optimal transport of nanomedicines within solid tumors.

Particle property	Vascular transport	Transvascular transport	Interstitial transport	Cellular uptake	Optimal overall condition
Size	> 12 nm and < 200 nm	> 12 nm < 60 nm	> 5 nm < 50 nm	~ 50 nm	12–50 nm
Surface charge	Neutral	Cationic	Neutral	Cationic	Neutral/slightly positive
Shape	Any shape	Elongated (high aspect ratio)	Elongated (high aspect ratio)	Not conclusive	Elongated